Effect of Bentonite on the Physical Properties and Drug-Release Behavior of Poly(AA-*co*-PEGMEA)/Bentonite Nanocomposite Hydrogels for Mucoadhesive

Wen-Fu Lee, Yung-Chu Chen

Department of Chemical Engineering, Tatung University, Taipei, Taiwan, Republic of China

Received 21 March 2003; accepted 26 August 2003

ABSTRACT: A series of nanocomposite hydrogels for mucoadhesive were prepared from acrylic acid, poly(ethylene glycol) methyl ether acrylate, and intercalated bentonite clay by photopolymerization. The microstructures were identified by X-ray diffraction (XRD). Results showed that the swelling ratio for the present nanocomposite hydrogels decreased with an increase of bentonite, whereas the gel strength and Young's modulus of the present gels increased with an increase of bentonite. However, the adhesive force of the present gels did not decrease with an increase of bentonite. XRD results indicated that the exfoliation of bentonite was achieved in the xerogels and swollen gels. Finally, the drug-release behaviors for these gels were also assessed.
 J Appl Polym Sci 91: 2934–2941, 2004

Key words: acrylic acid; bentonite; poly(ethylene glycol) methyl ether acrylate (PEGMEA); nanocomposite hydrogels; mucoadhesive

INTRODUCTION

Bioadhesion is defined as the adhesion of a polymer and a biological structure and is significant for many hard and soft tissue applications. The term mucoadhesive is applied when the substrate is mucus.[1] Some researchers have concluded that polymer characteristics necessary for mucoadhesive can be summarized as follows: strong hydrogen-bonding groups (–OH, –COOH), strong anionic charge (COO^-, SO^{3-}), high molecular weight, sufficient chain flexibility, and surface energy properties favoring the spread onto mucus.[2,3] In recent years, drug-delivery systems, using mucoadhesive drug carriers, have become increasingly important because of their ability to adhere to mucosal surfaces of the buccal cavity and skin, thereby increasing therapeutic efficiency.[4,5] Typical polymers that have been used as mucoadhesive drug carriers include poly(acrylic acid) (PAA), poly(methacrylic acid), carboxymethyl cellulose, and hydroxypropyl methylcellulose.[6,7] A wide range of polymers, both natural and synthetic, has been studied for their potential use as mucoadhesives.[8–12] Among the investigated polymers, PAA and its lightly crosslinked polymer have been shown to be good mucoadhesives because of their hydrophilic nature, negative charge, and high flexibility.[9,13]

Bentonite is a natural clay mineral, which has large layer space and some excellent properties such as good water absorption, swelling, adsorbability, cation exchange, and drug-carrying capability.[14,15] The present work focuses mainly on clay/polymer nanocomposites based on clays with a layered structure, among which bentonite is best known. By using a swelling agent for cation exchange to replace the metallic cations on the surface by amino groups ($–NH_2$), the swelling of the clay structure along the *z*-axis direction increases the interlayer distance in the *z*-axis.

Through polymerization, binding, or kneading, exfoliation of the silicate layers in the clay structure occurs with nanoscale dispersion along with the polymer substrate to form clay/polymer nanocomposites.[16] Recently, Messersmith and Znidarsich[17] first reported stimuli-responsive polymer hydrogel–clay composites by direct copolymerization of *N*-isopropyl acrylamide (NIPAAm) with methylenebisacrylamide in aqueous suspensions of Na–bentonite. Liang et al.[18] demonstrated a new approach to prepare a thermosensitive polymer–clay nanocomposite with enhanced temperature response based on organically modified clay/poly(PNIAAm) nanocomposites. The effect of montmorillonite (MMT) on the swelling behavior and drug-release behavior of the NIPAAm and MMT nanocomposite hydrogels was investigated in our previous study.[19]

In this study, a series of hydrogels used for mucoadhesion were prepared from acrylic acid (AA), poly(ethylene glycol) methyl ether acrylate (PEGMEA), and bentonite by photopolymerization. The effect of bentonite content in organoclay–polymer nanocom-

Correspondence to: W.-F. Lee (wflee@ttu.edu.tw).
Contract grant sponsor: Tatung University, Taipei, Taiwan; contract grant number: B90-1413-01.

Journal of Applied Polymer Science, Vol. 91, 2934–2941 (2004)

TABLE I
Feed Compositions, Yield, and Equilibrium Swelling Ratio of the Hydrogels

Sample code	AA (mol %)	PEGMEA (mol %)	NMBA (mol %)	Bentonite (mol %)	DEAP (mol %)	Yield (%)	Q (g/g) (%)
P0	90	10	0.1	0	0.1	95.3	1.32 (0)
P1	90	10	0.1	1	0.1	96.5	1.28 (3.0)
P3	90	10	0.1	3	0.1	91.3	1.23 (6.8)
P5	90	10	0.1	5	0.1	91.8	1.19 (9.8)
P7	90	10	0.1	7	0.1	90.4	1.16 (12)

posite hydrogels on the swelling behavior and physical properties in saline solution was investigated. In addition, a further objective in this article was to investigate the effect of the bentonite in the present gels on the drug-release behavior for drugs with different charges.

EXPERIMENTAL

Materials

Acrylic acid (AA), and diethoxyacetophenone (DEAP) as a photoinitiator, were purchased from Fluka Chemie (Buchs, Switzerland). 3-Acrylamidopropyl trimethylammonium chloride (TMAACl) was purchased from TCI (Tokyo, Japan). Ultrapure water with a conductivity of 18 S/cm was used in all experiments. The cation-exchange capacity (CEC) of the bentonite clay was about 120 meq/100 g. Poly(ethylene glycol) methyl ether acrylate (PEGMEA, M_n = 454) and *N*,*N*-methylenebisacrylamide (NMBA, M_n = 156) as a crosslinker were purchased from Aldrich Chemical and Sigma Chemical (St. Louis, MO), respectively. Vitamin B2, vitamin B12, crystal violet (CV), and phenol red as model drugs were obtained from Sigma and Fluka, respectively. All solvents and other chemicals were used as received, except acrylic acid (AA), which was purified by vacuum distillation at 29°C/6 mmHg.

Purification of bentonite

A 30-g sample of clay was suspended in 1000 mL of NaCl solution with a concentration of 1*M*. The suspension solution was stirred for 10 h at 70°C, after which the suspension solution was centrifuged: the purified bentonite precipitated as a yellow gel. The purified bentonite was washed four times with water to remove excess NaCl. Finally, the obtained bentonite was dried in a vacuum oven at 35°C for 3 days.

Intercalation of bentonite

The suspension solution containing 5 g of bentonite and 1.64 g of TMAACl was mixed in 500 mL of water. The suspension solution was stirred at 70°C for 24 h. Then, the intercalated bentonite was separated by centrifugation and washed with large volumes of water to remove nonintercalated TMAACl and residual NaCl. The sample was dried in a vacuum oven.

Preparation of AA/PEGMEA

Monomers, 90 mol % of AA, and 10 mol % of PEGMEA were weighed and mixed in a 20-mL sample vial. To this solution, 0.1 mol % of NMBA, 0.1 mol % of DEAP, and intercalated bentonite, with various ratios based on monomer weight, were then poured in and mixed thoroughly. The mixture was then injected into the space between two glass plates with a 1-mm silicone rubber as a spacer. Polymerization was carried out by exposing the monomer solution to UV irradiation for 10 min. After gelation was completed, the gel membrane was cut into disks, 10 mm in diameter, and immersed in an excess amount of deionized water for 3 days to remove residual components, and dried in a 50°C vacuum oven for 1 day. The feed compositions, yield, and equilibrium-swelling ratio of the nanocomposite hydrogels are listed in Table I.

Equilibrium swelling ratio measurement

The dried gels were immersed in 10 mL of 0.9 wt % NaCl at 25°C until swelling equilibrium was attained. The weight of the wet sample (W_t) was determined after removing the surface water by blotting with filter paper. Weight of the dry sample (W_d) was determined after drying the gel in a vacuum oven for 2 days. The equilibrium swelling ratios (Q) of the gels were calculated using the following equation:

$$Q = (W_t - W_d)/W_d \quad (1)$$

Swelling kinetics measurement

The swelling ratio was obtained by weighing the initial and swollen samples at various time intervals. The amount of water absorbed (W_t) was reported as a function of time, and the equilibrium absorption at infinitely long time was designated as W_∞. The following equation can be used to calculate the diffusion coefficient D for $W_t/W_\infty \leqq 0.8$[20]:

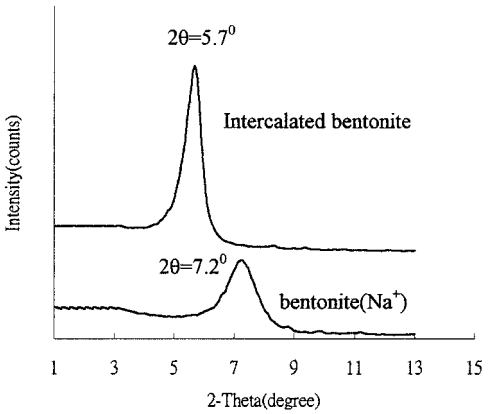

Figure 1 XRD patterns of Na–bentonite and intercalated bentonite.

$$W_t/W_\infty = (4/\pi^{0.5})(Dt/L^2)^{0.5} \quad (2)$$

where t is the time and L is the initial thickness of the dried gel. To investigate the diffusion model of the gel, the initial swelling data were fitted to the exponential heuristic equation for $W_t/W_\infty \leqq 0.6$.[21,22]

$$W_t/W_\infty = Kt^n \quad (3)$$

where K is a characteristic constant of the gel and n is a characteristic exponent of the mode transport of the penetrate.

pH sensitivity of nanocomposite hydrogel

A series of pH buffer solutions (citric acid/Na_2HPO_4) were prepared and adjusted to a constant ionic strength of 0.6*M* by adding NaCl. The preweighed dried gels were immersed in 10 mL of prepared buffer solutions to swell. The equilibrium–swelling ratio of gels in each pH solution was calculated using eq. (1).

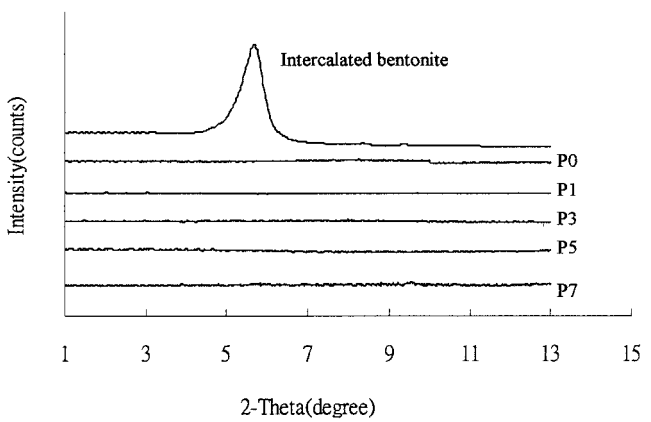

Figure 2 XRD patterns of intercalated bentonite and various dried gel samples.

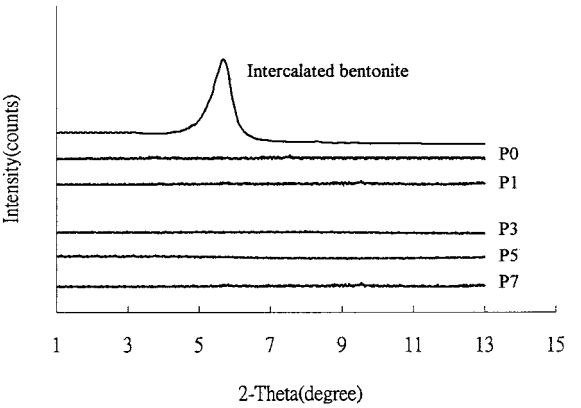

Figure 3 XRD patterns of intercalated bentonite and various samples in the swollen state.

Physical properties measurement

The gel strength of these samples was measured by uniaxial compression experiment with a universal tester (Lloyd LRX; J. J. Lloyd, Poole, UK). Equation (4) was used to calculate the shear modulus (G):

$$\tau = F/A = G(\lambda - \lambda^{-2}) \quad (4)$$

where τ is the compression stress, F is the compression load, A is the cross-sectional area of swollen gels, and λ is the compression strain (L/L_0). At low strains, a plot of τ versus $-(\lambda - \lambda^{-2})$ would yield a straight line whose slope is G. The effective crosslink density (ρ) can be calculated from the G and polymer volume fraction (ν_2) as follows:

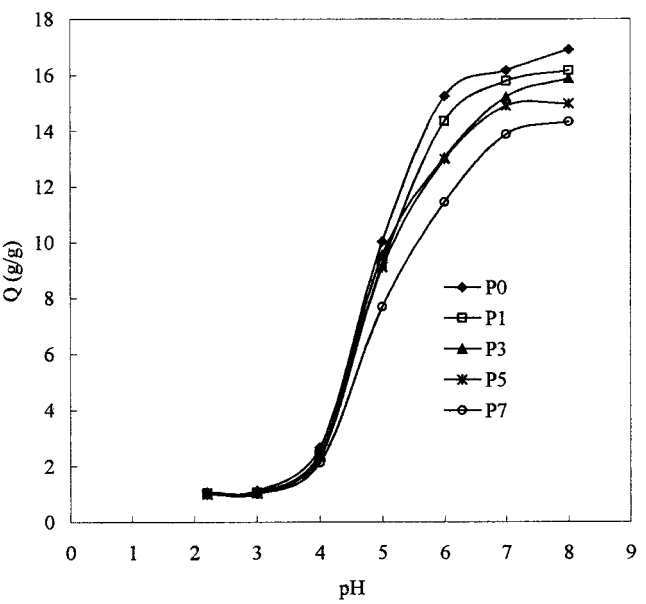

Figure 4 Effect of pH on equilibrium swelling for the AA/PEGMEA/bentonite gels in different buffer solutions.

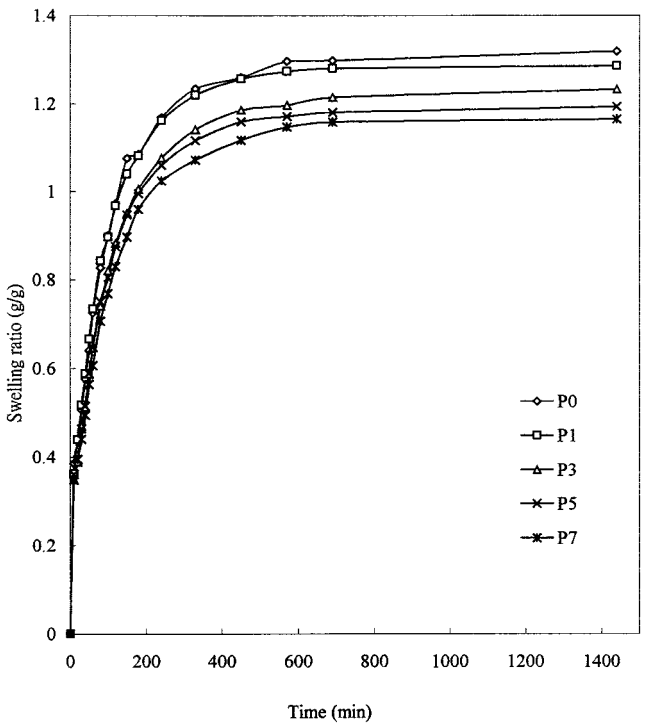

Figure 5 Swelling ratio as a function of time for the hydrogels in saline solution at 25°C.

$$\rho = G/\nu_2^{1/3}RT \quad (5)$$

where R is the ideal gas constant and T is the absolute temperature.

Assessment of adhesive force

The force detection system consisted of a precision load cell and roller with universal tester (Lloyd LRX). The nanocomposite gels were cut into the dimension of 3 × 1 cm (thickness: 1 mm), after which they were brought in contact with PET film on the roller. Peel strength was performed with a constant speed of 30 mm/cm and the force required to fracture the mucoadhesive bond was recorded.

Drug-release experiment

The model solutes used in drug release experiments were vitamin B2, vitamin B12, crystal violet (CV), and phenol red. The dry gels were equilibrated in 30 mg drug/10 mL of deionized water at 25°C for 2 days to load the drugs into the gels. The drug-release experiments were carried out by transferring previously incubated drug gels into 10 mL 0.9 wt % saline solution at 32°C. The gels were repeatedly removed and transferred into 10 mL fresh saline solution at each fixed time interval. The released drugs were analyzed by ultraviolet spectrophotometer (Jasco V530; Tokyo, Japan) for vitamin B2 at 445 nm, for vitamin B12 at 360 nm, for CV at 598 nm, and for phenol red at 430 nm, respectively.

X-ray diffraction analysis

Powder XRD analyses were performed by using a MAC Sienco X-ray powder diffractometer with Cu anode (model M21X), (Osaka, Japan), running at 40 kV and 30 mA, scanning from 1 to 13° at 3°/min. The structure of the clay was determined at different stages of the nanocomposite synthesis. The clay powders were mounted on a sample holder with a large cavity, and a smooth surface was obtained by pressing the powders with a glass plate. Analyses of the organoclay swollen in the gels were performed by spreading the mixture onto a gel membrane disc (50 mm diameter, 0.5 mm thick) used as a sample holder. It was designed so that a maximum surface could be irradiated at low angle, giving an optimum intensity to the XRD signal. The nanocomposite plates produced during the molding process had a fairly smooth surface.

RESULTS AND DISCUSSION

Identification of the nanocomposite hydrogels

The XRD patterns of various samples are plotted in Figure 1. A typical XRD pattern of bentonite, with a strong peak corresponding to a basal spacing of 12.3 Å, is shown in Figure 1. After treatment with TMAACl the peak was shifted to a low angle, corresponding to a basal spacing of 15.5 Å. This shows that the short chain, acrylamidotrimethylammonium ion, was intercalated between the layers during the cation-exchange process, adopting a lateral bilayer structure. After po-

TABLE II
Some Fundamental Properties of Poly(AA-*co*-PEGMEA)/Bentonite Nanocomposite Hydrogels

Sample code	$D \times 10^7$ (cm^2/s)	n	$K \times 10^2$	G (g/cm^2)	$\rho \times 10^{-4}$ (mol/cm^3)	Adhesive force (N/cm^2)
P0	0.27	0.20	7.6	2202 ± 51	1.33 ± 0.54	0.226 ± 0.024
P1	0.25	0.17	8.8	3062 ± 45	1.76 ± 0.46	0.245 ± 0.003
P3	0.21	0.15	9.2	3621 ± 75	2.03 ± 0.18	0.231 ± 0.007
P5	0.19	0.12	10.8	3771 ± 64	2.14 ± 0.77	0.237 ± 0.013
P7	0.15	0.11	12.4	4818 ± 86	3.01 ± 0.73	0.224 ± 0.018

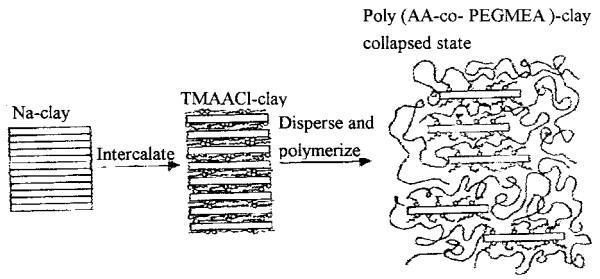

Scheme 1 *In situ* polymerization of poly(AA-*co*-PEGMEA)/bentonite nanocomposite hydrogels..

lymerization, both the dried gels and the swollen gels were also analyzed by XRD.

The XRD patterns of the various xerogels and swollen gels, shown in Figures 2 and 3, respectively, indicate that the diffraction peak disappears in all samples. This result confirms that the intercalated bentonite incorporated into the gels was exfoliated.

Effect of bentonite on the nanocomposite hydrogel properties

The effect of bentonite on some fundamental properties, such as equilibrium swelling ratio, adhesive force, gel strength, and drug release, for the present nanocomposite hydrogels was investigated.

Effect of bentonite on equilibrium swelling ratio

Some characteristics of the poly(AA-*co*-PEGMEA)/bentonite gels with various feed compositions are shown in Table I. The equilibrium–swelling ratios (Q) for the present hydrogels in Table I indicate that the greater the bentonite content in the gels, the lower the Q value of the gels (i.e., P0 > P1 > P3 > P5 > P7). This is because the original hydrophilic bentonite modified with TMAACl becomes a hydrophobic chain: it makes the nanocomposite hydrogels become more hydrophobic. Hence, the swelling ratio decreased (12%) with increase in the content of bentonite (7 mol %) in the gel.

Effect of ph on swelling ratio

The effect of pH on equilibrium–swelling ratio for the present nanocomposite hydrogels is shown in Figure 4. The results, shown in Figure 4, indicate that the higher the pH, the higher the swelling ratio. However, the gel transition in different pH solutions was not obviously affected by the addition of more bentonite in the gel. Although the gel transition did not change, the gels still possessed excellent pH response under high clay loadings. The gel transition for the present gels was at around pH = 5. Because AA is the main component in the present copolymeric gels, the swelling ratio increases with an increase of pH. The results shown in this figure indicate that, at lower pH (=2), the swelling ratio was the same but, at higher pH (=8), the swelling ratio increased with increase in bentonite content.

Effect of bentonite on the swelling kinetics

The swelling ratios as a function of time for the present gels in saline solution are shown in Figure 5. The n, K, and D values calculated from eqs. (2) and (3) are listed in Table II. The results show that the diffusion coefficients for the gels present in saline solution decrease with increase in bentonite content in the gel. Alfrey et al.[23] distinguished three classes of diffusion according to the relative rates of diffusion and polymer chain relaxation:

1. Fickian diffusion (Case I: $n < 0.5$), in which the rate of diffusion is much smaller than that of

TABLE III
Drug-Loading Amount and Fractional Release of Nanocomposite Hydrogels

Drug	Sample code				
	P0	P1	P3	P5	P7
CV					
Loading amount (ppm/g)	2434.26	2488.26	2589.6	2680.69	2788.44
Fractional release at 1440 min	15.5%	14.61%	13.87%	13.2%	12.7%
Phenol red					
Loading amount (ppm/g)	361.615	346.44	312.72	275.07	248.46
Fractional release at 1440 min	57%	62.4%	66.67%	74.27%	80.86%
Vitamin B12					
Loading amount (ppm/g)	686.4	706.89	741.67	782.2	829.43
Fractional release at 1440 min	74.7%	66.82%	58.63%	52.46%	48.92%
Vitamin B2					
Loading amount (ppm/g)	818.7	792.67	740.08	687.51	637.76
Fractional release at 1440 min	70.23%	66.48%	64.14%	62.58%	60.98%

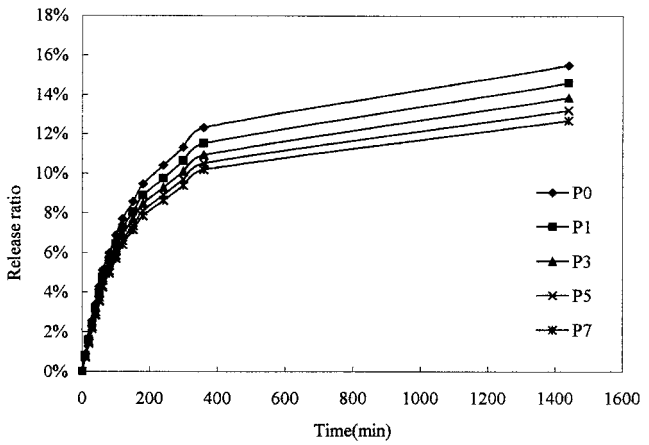

Figure 6 CV release profiles of AA/PEGMEA/bentonite gels at 32°C saline solution.

relaxation. In this case the system is controlled by a diffusion phenomenon.

2. Case II (n = 1.0) is the other extreme, in which the diffusion process is very fast compared to the relaxation process. The controlling step is the velocity of an advancing front, which forms the boundary between a swollen gel and a glassy core.
3. Non-Fickian diffusion (n = 0.5–1.0) describes those cases where the diffusion and relaxation rates are comparable. Hence, the results shown in Table II indicate that the transport mechanisms for the present nanocomposite hydrogels belong to Fickian diffusion.

Effect of bentonite on the adhesive force

The adhesive forces of the nanocomposite hydrogels are shown in Table II. The adhesive force was determined by measuring the force required to break the adhesive surface between the substrate (PET film) and the gels. The results show that the adhesive force for the present gels was not affected by the addition of bentonite in the gel.

Effect of bentonite on gel strength

The gel strength was assessed by the shear modulus (G), obtained from eq. (4). The results in Table II indicate that the G values increase with an increase of the content of bentonite. This result may be attributed to bentonite particles becoming exfoliated and dispersed at the nanoscale in the gel matrix. This occurrence could increase the particle surface area and result in an increase of the interaction between the gel matrix and bentonite dispersed phase.

The effective crosslink density (ρ) is defined as the concentration of elastically active chain (chains are deformed by an applied active stress) in the polymer network and is usually reported on the basis of moles of chain per cubic centimeter of dry polymer. The ρ values for the present gels can be obtained from eq. (5). The results shown in Table II indicate that the ρ values increase with increase in the bentonite content in the gel, which implies that the incorporation of the bentonite into the gel can enhance the chemical crosslinks between the matrix and dispersed phase. Because vinyl monomer, TMAACl, grafted onto the surface of the nanoclay layer, is a potential crosslinking point between the nanoclay layer and poly(AA-*co*-PEGMEA) matrix through *in situ* polymerization, the compatibility between these two phases can be improved. Thus, the well-dispersed nanoclay layers effectively enhance the gel strength and crosslinking density of the nanocomposites hydrogels (see Scheme 1).

Effect of bentonite on fractional drug release of different ionic drugs on the release behavior

In this study, because bentonite bears negative charges on the surface, the nanocomposite hydrogel possesses negative charges. The loading amount and fractional release of the model drugs in the present gels are shown in Table III. The drug release profiles of crystal violet (CV), phenol red, vitamin B12, and vitamin B2, in saline solution for the nanocomposite hydrogels at 32°C are shown in Figures 6–9, respectively.

The results of cationic CV solutes releasing from the gels in saline solution are shown in Figure 6. Because the charges of CV and gel are different, electrostatic attraction exists. Hence, the CV solute strongly binds on the anionic gels and it is difficult to release it out of the gel. For the P1 sample, the absorption concentration of CV per gram bentonite, based on P0 (as control

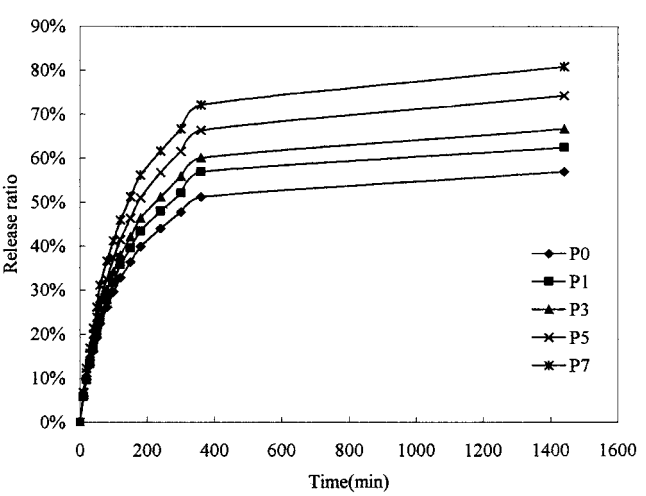

Figure 7 Phenol red release profiles of AA/PEGMEA/bentonite gels at 32°C saline solution.

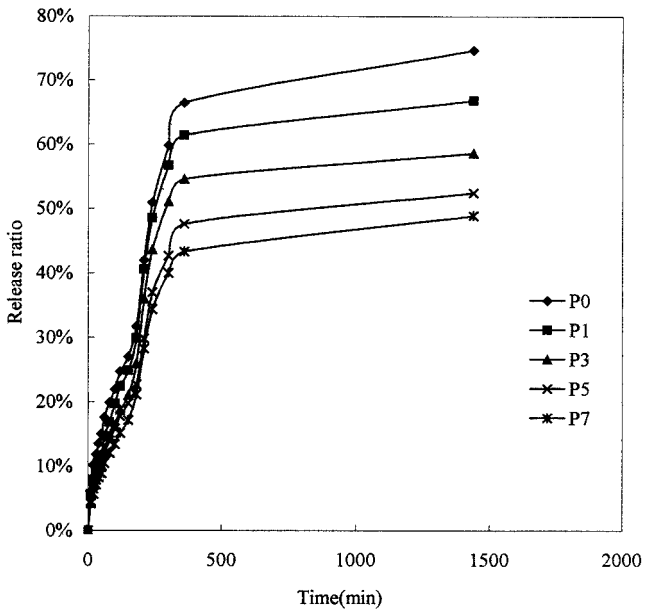

Figure 8 Vitamin B12 release profiles of AA/PEGMEA/bentonite gels at 32°C saline solution.

gel), is about 54 ppm/g. This can be observed from the loading amount of CV in the gels (see Table III). Hence, the fractional release of CV in the gels decreases with increase in bentonite content.

The results of anionic phenol red solute releasing from anionic gels are shown in Figure 7. The charges of the phenol red and the present hydrogel are the same, so the loading amounts of phenol red in the gels decrease with increase in bentonite. On the contrary, the fractional release of phenol red in the gels increases with increase in bentonite. This is because charge repulsion exists between the drug solute and gel: the solute is difficult to load into the gel but is easily released from the gel.

The results of zwitterionic vitamin B12 solute releasing from the gels in saline solution are shown in Figure 8. Vitamin B12 is a zwitterionic drug with anion (PO_3^-) and cation (Co^+). For vitamin B12, the negative charges in the gels are adsorbed onto the positive charged part of the drug molecule. For the P1 sample, the absorption concentration of vitamin B12 per gram bentonite, based on control sample P0, is about 20.5 ppm/g. Hence, although the loading amount of vitamin B12 in the gel increases with increase in bentonite, the fractional release of vitamin B12 in the gels decrease with increase in bentonite. This is because the nanocomposite hydrogel possesses negative charges and Co^+ of the vitamin B12 adsorbs only onto the surface of the gels.

The results of uncharged vitamin B2 solute releasing from the gels in saline solution are shown in Figure 9. Vitamin B2 is an uncharged small-molecule drug. The bonding force between vitamin B2 and gels is small, so the loading and release of vitamin B2 are mainly affected by the crosslink density (ρ) of the hydrogel. Hence, the results show that the loading amount of vitamin B2 in the gels decreases with an increase in bentonite, and the fractional release of vitamin B2 in the gels also decreases with an increase in bentonite.

From the above results, we find that the drug-release behavior in poly(AA-*co*-PEGMEA)/bentonite nanocomposite hydrogels is profoundly affected by the bentonite content, charge of drug solute, and interaction between gel and drug solute. These results conform to our previous studies in NIPAAm/montmorillonite hydrogels[19] and charge effects on drug-release behavior for ionic thermosensitive hydrogels.[24]

CONCLUSIONS

Poly(AA-*co*-PEGMEA)/bentonite nanocomposite mucoadhesive was successfully synthesized. Some conclusions can be made from the preceding discussion as follows: the greater the content of the bentonite, the lower the swelling ratio of the gels. The gel transition at various pH conditions was not affected by the content of bentonite in the gel. The XRD patterns showed that, in the xerogels and the swollen hydrogels, the bentonite clay was intercalated and exfoliated. The gel strength and crosslinking density of the gels were enhanced by adding bentonite into the gel composition, attributed to the chemical crosslinking formed between the gel matrix and bentonite dispersed phase through *in situ* polymerization. The main adhesive property is affected by acrylic acid, so the adhesive

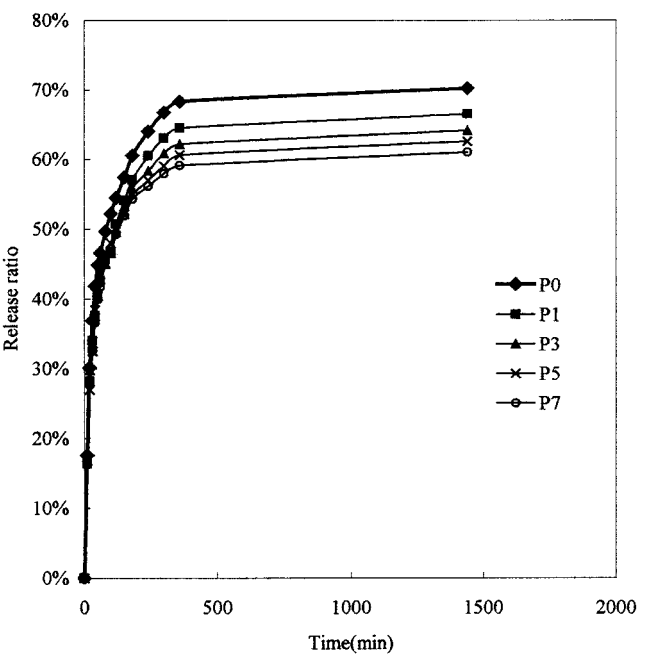

Figure 9 Vitamin B2 release profiles of AA/PEGMEA/bentonite gels at 32°C saline solution.

force is not significantly affected by the addition of bentonite.

The results of drug-release behaviors for different kinds of drugs showed that the drug-release behaviors were affected by different release factors, including the electrostatic attraction and repulsion between gel and drug, and the gel network. If the charges of the drug solute and hydrogel are different, electrostatic attraction exists between them and the drug strongly binds in the nanocomposite gels, so the release ratios are lower. On the contrary, if the charges of the drug solutes and hydrogel are the same, the release ratio of the gel is higher. The swelling ratios of the nanocomposite hydrogels indicate that the gel with higher swelling ratio can make uncharged drug solute release easily through the gel.

The authors gratefully acknowledge financial support of this research by the Tatung University, Taipei, Taiwan, under Grant B90-1413-01.

References

1. Shojaei, A. H.; Li, X. J Controlled Release 1997, 47, 151.
2. Mortazavi, S. A. Int J Pharm 1995, 124, 173.
3. Chickering, D. E.; Mathiowitz, E. J. Controlled Release 1995, 34, 251.
4. Florence, A. T.; Jani, P. U. Drug Saf 1994, 10, 233.
5. Hwang, S. J.; Park, H. Grit Rev Ther Drug Carrier Syst 1998, 15, 243.
6. Ahuja, A.; Khar, R. K.; Ali, J. Drug Dev Ind Pharm 1997, 23, 489.
7. Yang, X. J.; Robinson, R. In: Biorelated Polymers and Gels: Controlled Release Application in Biomedical Engineering; Okano, T., Ed.; Academic Press: London, 1998; pp. 135–192.
8. Gandhi, R. E.; Robinson, J. R. Ind J Pharm Sci 1988, 50, 145.
9. Ch'ng, H. S.; Park, H.; Kelly, P.; Robinson, J. R. J Pharm Sci 1985, 74, 399.
10. Kriaet, B.; Kissel, T. Int J Pharm 1996, 127, 135.
11. Leung, S. S.; Robinson, J. R. J Controlled Release 1990, 12, 187.
12. Lether, C. M.; Bouwstra, J. A.; Schacht, E. H.; Junginger, H. E. Int J Pharm 1993, 78, 43.
13. Park, H.; Robinson, J. R. Pharm Res 1987, 4, 457.
14. Macter, W. J.; Broussean, R. Cement Concrete Res 1990, 20, 891.
15. Akelah, A.; Moet, A. J Appl Polym Sci Appl Polym Symp 1994, 55, 153.
16. Kornmann, X.; Berglund, L. A.; Sterte, J. Polym Eng Sci 1998, 38, 1351.
17. Messersmith, P. B.; Znidarsich, F. In: Nanophase and Nanocomposite Materials II, MRS Symposium Proceedings 457; Komarneni, S.; Parker, J. C.; Wollenberger, H. J., Eds.; Materials Research Society: Pittsburgh, PA, 1997; p. 507.
18. Liang, L.; Liu, J.; Gong, X. Langmuir 2000, 16, 9895.
20. Kabra, B. G.; Gehnke, S. W.; Hwang, S. T. J Appl Polym Sci 1991, 42, 2409.
19. Lee, W. F.; Fu, Y. T. J Appl Polym Sci 2003, 89, 3652.
21. Franson, N. M.; Peppas, N. A. J Appl Polym Sci 1983, 28, 1299.
22. Korsmeyer, R. W.; Merrwall, E. W.; Peppas, N. A. J Polym Sci Polym Phys Ed 1986, 24, 109.
23. Alfrey, T.; Gurnee, E. F.; Lloyd, W. G. J Polym Sci C 1996, 12, 249.
24. Lee, W. F.; Chiu, R. J Mater Sci Eng 2002, C20, 161.